LETTERS

# Optical manipulation of nanoparticles and biomolecules in sub-wavelength slot waveguides

Allen H. J. Yang[1], Sean D. Moore[2], Bradley S. Schmidt[3], Matthew Klug[2], Michal Lipson[3] & David Erickson[2]

**The ability to manipulate nanoscopic matter precisely is critical for the development of active nanosystems. Optical tweezers[1–4] are excellent tools for transporting particles ranging in size from several micrometres to a few hundred nanometres. Manipulation of dielectric objects with much smaller diameters, however, requires stronger optical confinement and higher intensities than can be provided by these diffraction-limited[5] systems. Here we present an approach to optofluidic transport that overcomes these limitations, using sub-wavelength liquid-core slot waveguides[6]. The technique simultaneously makes use of near-field optical forces to confine matter inside the waveguide and scattering/adsorption forces to transport it. The ability of the slot waveguide to condense the accessible electromagnetic energy to scales as small as 60 nm allows us also to overcome the fundamental diffraction problem. We apply the approach here to the trapping and transport of 75-nm dielectric nanoparticles and λ-DNA molecules. Because trapping occurs along a line, rather than at a point as with traditional point traps[7,8], the method provides the ability to handle extended biomolecules directly. We also carry out a detailed numerical analysis that relates the near-field optical forces to release kinetics. We believe that the architecture demonstrated here will help to bridge the gap between optical manipulation and nanofluidics.**

In a series of recent articles, Psaltis *et al.*[9] and Monat *et al.*[10] describe the enormous potential of integrating optical and microfluidic elements into 'lab-on-a-chip' devices, particularly in improving fluid and particle manipulations. Traditionally accomplished through direct particle manipulation with laser tweezers[1–3,11] or indirectly using optically induced microfluidic effects[12,13], the precision with which particles can be manipulated with these techniques makes them particularly useful for applications ranging from flow cytometry[3,14] to self-assembly[15]. Fundamentally, however, these free-space systems are limited in two ways. First, diffraction limits how tightly the light can be focused and thereby limits the overall strength of the trap. Second, the trapping region has a very short focal depth, preventing the continuous transport of nanoparticles by means of radiation pressure.

To improve trapping stability, a number of near-field methods have recently been developed[16–18]. Examples are the use of interfering Gaussian beams reflected off a prism surface to sort 350-nm polystyrene beads[19], and the use of localized plasmonic resonances in surface-bound metallic nanostructures to trap 200-nm dielectric particles[4]. Waveguide-based optical transport[20,21] is analogous to these near-field methods in that the evanescent field extending into the surrounding liquid serves to attract particles to the waveguide. However, particles also experience photon scattering and absorption forces which propel them along it for a distance limited only by the losses in the system. Recent efforts in this area have demonstrated the sustained propulsion of dielectric microparticles[20,22], metallic nanoparticles[23,24] and cells[25]. The limitation that prevents these systems from manipulating smaller matter, including biomolecules, is that the particles only interact with the small portion of total transported light because most of it is confined within the solid core of the waveguide.

Recently Almeida *et al.*[6] developed a nanophotonic structure, known as a slot waveguide, that can overcome this challenge. Illustrated in Fig. 1, the slot waveguide comprises a nanoscale slot sandwiched between two materials of much higher refractive index. As shown in Fig. 1b, there exists a pseudo-transverse-electric (TE) mode that has a large electric field discontinuity at the horizontal boundaries of the slot region. The result is a high-intensity eigenmode in the slot making the majority of the optical energy accessible within the low-index fluid region. Here we demonstrate the use of these sub-wavelength-scale slot waveguides for optical capture, trapping and transport of both dielectric nanoparticles and λ-DNA molecules. We can achieve stable trapping of particles as small as 75 nm, representing some of the smallest dielectric matter ever trapped or transported using such a system. In addition to the experimental results, we also present an examination of the effect that the presence of a particle has on the optical mode, details of the trap strength and stiffness in comparison with other techniques, and a unique stability analysis descriptive of the release kinetics for particles near the stability point.

As shown in Fig. 2a (see also Supplementary Movies 1 and 2), we are able to capture and stably trap polystyrene nanoparticles (refractive index $n = 1.45$) with diameters of 75 nm and 100 nm in slot waveguides with widths of 100 nm and 120 nm, respectively. In all cases the optical power at the exit of the fibre used to couple light into the waveguide was less than 300 mW, the excitation wavelength was $\lambda = 1{,}550$ nm, and the trapping used TE polarization. Experimental details are available in the Supplementary Information. The first movie (Supplementary Movie 1) illustrates our ability to capture and accumulate flowing particles in the slot waveguide for indefinite periods of time and release them by either reducing the optical power or switching the polarization. Excitation of the slot waveguides using transverse-magnetic (TM) polarization required three to five times as much power to obtain stable trapping, so switching polarization also tended to break the trap. The microfluidic flow serves to transport the particles to the waveguide but does not have a role in the trapping itself. This is indicated by the fact that the trap breaks on removal of the optical excitation in the above experiments.

The second movie (Supplementary Movie 2) illustrates the dynamics of the capture of flowing particles in a trap near the stability point, where the random thermal energy in the system is of the same order as the amount of work required to break the trap[26]. The average retention time in such a trap is a statistical process governed by the release kinetics of the system, which in turn is governed by the trap strength, its stiffness and the location on the waveguide where the particle is trapped (as will be described below). In the experiment

[1]School of Chemical and Biomolecular Engineering, [2]Sibley School of Mechanical and Aerospace Engineering, [3]School of Electrical and Computer Engineering, Cornell University, Ithaca, New York 14853, USA.

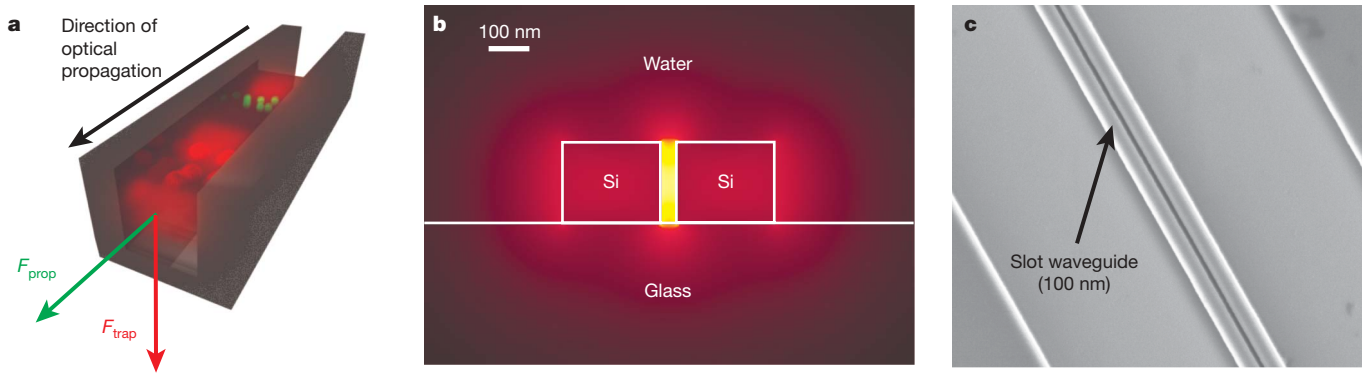


**Figure 1 | Nanoscale optofluidic transport.** **a**, Schematic illustrating the transport of two different sizes of nanoparticles in a slot waveguide. The force $F_{prop}$ represents the radiation pressure force responsible for optofluidic transport, and $F_{trap}$ is the trapping force that holds nanoparticles within the slot region. **b**, Mode profile for a silicon-on-insulator 40-nm slot waveguide immersed in water, calculated using a finite-element simulation package. The main trapping region is in the high-intensity slot mode, although alternate trapping locations are located on the sides of the waveguide, where there are two decaying evanescent modes. **c**, Scanning electron microscope image of 100-nm slot waveguide structure

shown, the nanoparticles are flowing by in the microchannel at an average speed of 80 μm $s^{-1}$ and, as can be seen, the number of particles that are captured is low (less than 25%) in comparison with those that flow by. The reason for the low capture rate is that to be trapped, a particle must be on a streamline that passes through the evanescent field. This is analogous to a situation in which a flowing particle must pass through the focal point of a free-space optical tweezer in order to be trapped, and is not an inherent limitation of our system. The capture rate can be increased by decreasing the channel size, reducing the flow rate or increasing the optical power.

As mentioned above, an advantage of this approach is the ability not only to capture nanoscopic matter but to transport it optically. This capability is important for the development of active nano-assembly techniques and for optically driven bioanalytics[27]. From Rayleigh theory it is well known that the radiation-pressure-based transport velocity of a dielectric nanoparticle is proportional to the local intensity and scales with the fifth power of particle radius[28]. As such it is extremely difficult to optically transport very small matter unless very high optical intensities can be achieved. As shown in Fig. 2b (and Supplementary Movie 3), using our slot waveguide system we have been able to demonstrate optical propulsion of 100-nm particles at an average speed of 1.5 μm $s^{-1}$ (using 250 mW optical power measured at the exit of the fibre). Because the propulsion velocity is inversely proportional to the fourth power of wavelength, one method by which the transport velocity could be increased is by using a different high-refractive-index material that is transparent at lower wavelengths.

Nanoscopic dielectric particles can be considered as coarse approximate models for biological species such as viruses and very small bacteria. Of perhaps greater interest is the ability to capture and optically confine individual biomolecules. As shown in Fig. 3 (and Supplementary Movie 4) we have been able to capture from solution and stably trap individual strands of YOYO-1 tagged λ-DNA molecules 48 kilobases long. As in previous cases, trapping was accomplished using 250 mW of input optical power at a wavelength of 1,550 nm; in this case, however, we used a 60-nm slot waveguide. As can be seen in the second half of the movie, when the power is removed the DNA strands are released. These experiments were done under pH conditions in which the DNA is reported to be in a partially extended state[7]. Although others have demonstrated optical trapping of λ-DNA at pH levels at which the molecule is known to be in a supercoiled state[7,8], it has proved difficult to trap partially extended molecules because the focal point of a tightly focused tweezer can only interrogate a small portion of the molecule. The slot waveguide technique allows us to trap extended molecules, as the confinement force is equivalently applied along a line rather than at a point. Further development of the transport technique may also allow us to develop new biomolecular separation mechanisms or new methods of interrogating single molecules for rapid sequencing[29] or direct haplotyping[30].

To characterize the trapping stability, stiffness and release kinetics better, we have carried out a detailed three-dimensional numerical analysis of the system. Referring back to Fig. 2, although most of the particles were observed to be trapped in the high-intensity slot region, trapping was also observed along the sides of the slot waveguide

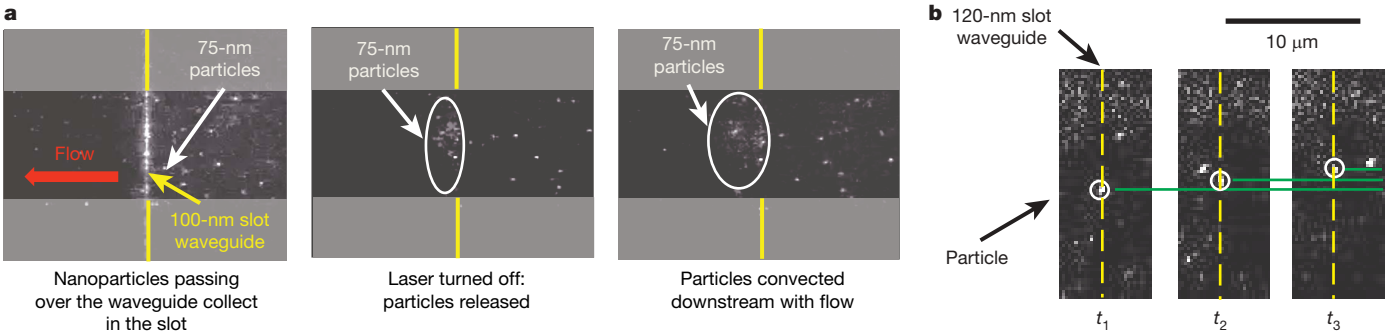


**Figure 2 | Trapping and transport of dielectric nanoparticles in a slot waveguide.** Movies illustrating nanoparticle capture, transport and release are included in the Supplementary Information. **a**, Waveguide is optically excited while 75-nm polystyrene nanoparticles flow in the overlying microchannel over 100-nm slot waveguides. Over time, particles collect in the slot and also on the sides of the waveguide. At $t = 0$, the laser source is removed and particles are released from the waveguide. Immediately after release, a 'cloud' of particles forms as the particles leave their trapping sites and the released particles are carried down the channel by the fluid flow. **b**, Trapped 100-nm nanoparticles in 120-nm slot waveguides are transported a short distance by radiation pressure. Time-lapse images are cropped from images taken using a SensiCam CCD camera with contrast and brightness adjustments to the entire image. The cropping location is the same in each time-lapse image.

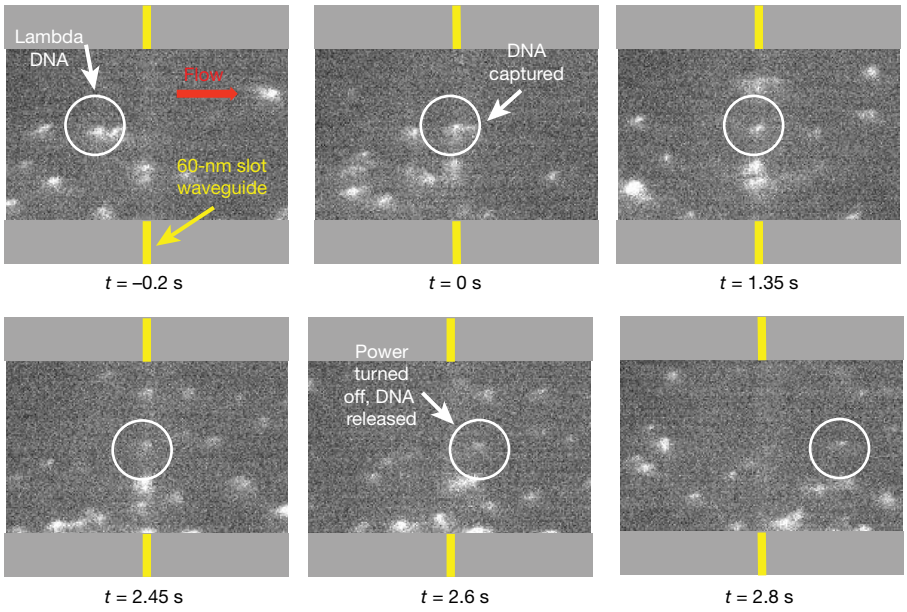


**Figure 3 | Capture and trapping of λ-DNA.** Movies illustrating the DNA capture and release are included in the Supplementary Information. Images show individual YOYO-tagged 48-kilobase λ-DNA flowing over an optically excited 60-nm-wide slot waveguide. At time $t = 0$ the encircled DNA is trapped. In this case the DNA is released at the 2.6-s mark and flows downstream. Supplementary Movie 4 shows the collection of DNA molecules over time and their release in response to removal of the optical excitation. Trapping conditions are identical to those used for the nanoparticle experiments shown in Fig. 2. Time-lapse images are cropped from images taken using a SensiCam CCD camera with contrast and brightness adjustments to the entire image. The cropping location is the same in each time-lapse image.

structure. Because the trap strength is related to the local optical field intensity, we can compare the behaviours of particles trapped in the two different regions to gauge the effect on trapping stability. To do this, we used a finite-element simulation to calculate the relative trapping force for a side-trapped particle in comparison with one trapped in the slot, shown in Fig. 4a, b. As can be seen, the trapping force for side-trapped particles is much smaller, and as a result less work energy is required to exceed the trapping release barrier. This

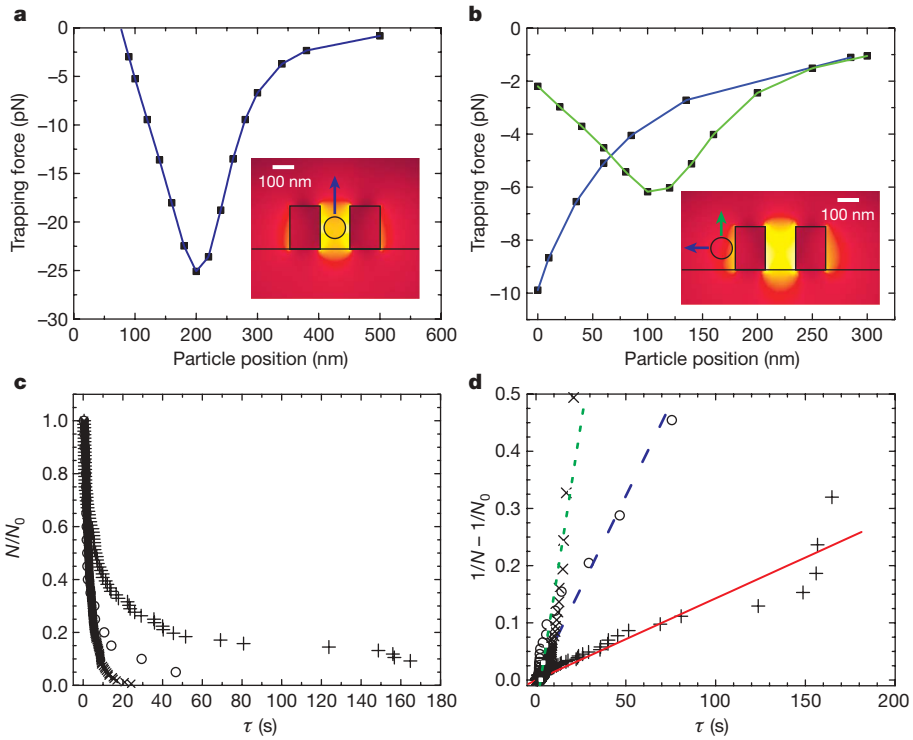


**Figure 4 | Trapping forces on particles trapped inside and outside the slot waveguide, and analysis of particle release kinetics.** The work required to release a particle from the trap is found by integrating the force curves from a particle's stable trapping position to infinity. Inset images show the calculated electric field distribution with the particle in the two stable trapping positions. The arrows indicate the direction of release. **a**, Trapping force for a 100-nm particle in a 120-nm slot plotted against its position relative to the height of the slot waveguide. The particle position is measured as the distance of the particle centre from the bottom of the 200-nm-tall slot waveguide. The trapping force reaches a maximum at the point where the field gradient is strongest at the entrance to the slot waveguide. **b**, Trapping force for a 100-nm particle side-trapped in the same structure with two possible release paths. Particle position is measured as the deviation of the particle centre from its most stable position. The blue line corresponds to a particle being pushed off the waveguide by an external force, and the green line corresponds to a particle being lifted up off the waveguide. The trapping forces listed are normalized to 1 W of guided power. **c**, Experimental data for $N/N_0$ plotted against normalized time, $\tau$. Particles trapped in the slot are represented by crosses, side-trapped particles are represented by circles, and DNA by × signs. The quantity $N/N_0$ represents the relative 'concentration' of particles trapped on the waveguide. **d**, Plot of $F(N)$ (see Supplementary Information) for a second-order rate law $(1/N - 1/N_0)$ versus $\tau$. The same symbols are used here as in **c**. The lines represent linear fits to the data, from which the release rate constant can be obtained. In this case sharper slopes represent a higher release rate and therefore a less stable trap.

provides an avenue to differentiate the two situations, as we would expect side-trapped particles to be released more easily than their slot-trapped analogues. Figure 4a, b also illustrates that the optical mode of the slot waveguide is not greatly perturbed by the presence of the particle in either position.

Because the direction of trap release is in the vertical direction, and because of the physical confinement provided by the channel walls and the fact that the trapping force does not vary along the length of the waveguide, it is difficult to extract quantitative values for the trapping stability experimentally. From the numerical computations, however, we can estimate the trap stiffness from the slope of the force-distance curve as being 0.2 pN per nanometre for a 100-nm nanoparticle at 1-W excitation power. Although a direct comparison is difficult, this is significantly higher than previously described for larger particles using other near-field techniques (see Grigorenko *et al.*[4] who reported a 0.013 pN nm$^{-1}$ stiffness for a 200-nm bead).

As described in previous analytical work[26], for a particle in an optical near field, there is a finite amount of work energy required to remove a particle from a stably trapped location to one where the trap no longer has any influence. When trapping is relatively weak and the particles small, the random thermal energy in the system will eventually exceed this work and the particle will be released. In such cases, the work energy is analogous to an activation energy barrier that impedes the release of particles from the waveguide, and the kinetic behaviour is similar to molecular desorption from a surface (see Supplementary Information for the theoretical basis). Understanding how related parameters such as slot width, particle composition and particle size affect the release rate of trapped nanoparticles yields information necessary for the engineering of robust, stable slot transport devices.

We carried out a large number of trapping experiments for nanoparticles trapped inside the slot, nanoparticles trapped outside the slot, and the trapped DNA. Trapping was done near the stability point such that the targets would self-release from the waveguide structure. Figure 4c shows a plot of the total number of trapped targets on the waveguide as a function of normalized time. The average release time for particles trapped inside the slot is larger than that for those trapped outside, suggesting greater stability, consistent with our earlier numerical predictions. The trapping stability is related to a kinetic constant, $k$, which can be obtained by plotting the above data as a function of reduced time for an appropriate rate law (see Supplementary Information). In Fig. 4d we see that side-trapped particles have a larger rate constant, suggesting that the release (desorption) is faster and a lower work energy is required for release. It is not yet clear why the release process seems to have a second-order rate, but we believe that it results from the exponential decay of the electromagnetic trapping force coupled with hydrodynamic drag. DNA shows a lower stability than the polystyrene nanoparticles, probably because of the extended conformation that it obtains during trapping. As the trapping stability is likely to be strongly dependent on molecular conformation, analysis of the release kinetics in such systems may result in a new method of single-molecule analysis.

Sub-wavelength slot waveguides such as those used in this work can be integrated into lab-on-a-chip platforms using existing manufacturing techniques. They allow discrete optical manipulation and transport of nanoscopic objects with greater precision than is available with existing approaches. The fusion of nanofluidics and optical manipulation in this manner could lead to new methods of bioanalysis and directed assembly.

## METHODS SUMMARY

We fabricate the slot waveguide chips using electron beam lithography. After experimental use, the chips are cleaned using Nanostrip, and scum is removed by using a reactive ion oxygen plasma etching process. The total width of the waveguides is 450 nm with slot widths ranging from 60 nm to 120 nm. The slot waveguides are transitioned to nanotaper devices clad in silicon oxide to increase the coupling efficiency. The laser source is a tunable 1,550-nm laser that runs to a tapered lensed fibre, using the same set-up previously used for our SU-8 waveguide experiments[20].

The particle solution consists of suspended fluorescent polystyrene nanoparticles 75 nm and 100 nm in diameter (Duke Scientific) with refractive index $n = 1.574$ in a 100 mM phosphate buffer solution. The particles have a dispersity in diameter of about 10%. The high ionic concentration of the buffer solution suppresses electrostatic interactions in the system and maintains a constant pH during experiments. We add 1%-by-volume Triton X-100 non-ionic surfactant to the particle solution to prevent aggregation of the nanoparticles and to limit adhesion of particles to the surface of the devices and PDMS microchannels.

The experiments use devices that are bonded to a PDMS microchannel 100 μm wide and 5 μm tall. The fluidics are driven using an adjustable air-pressure system designed to maintain a constant pressure to the device. The power output of the fibre during the trapping experiments was set from 250 to 300 mW. Particle trapping was confirmed by counting immobilized particles and counting the number of released particles. We determined particle velocity measurements and particle trapping times by using the ImageJ particle tracking software. Images of the experiments were captured at a rate of 55 ms per frame using a SensiCam CCD camera.

As mentioned in the main text, we carried out experiments demonstrating λ-DNA trapping using the technique described above, with the exception of the smaller 60-nm-wide slot waveguide. The λ-DNA molecules (New England BioLabs) were stained with YOYO-1 intercalating dye (Molecular Probes) so that they could be observed using traditional fluorescence microscopy. The buffer consisted of 10 mM Tris Base (J.T. Baker), 1 mM EDTA (Fisher), and 10 mM sodium chloride (Mallinckrodt) at a pH of 7.8. Poly(*n*-vinylpyrrolidone) (PVP, Sigma) 2% (by weight) was added to reduce unspecific binding of DNA to channel walls.

**Received 31 May; accepted 21 October 2008.**


1. Grier, D. G. A revolution in optical manipulation. *Nature* **424,** 810–816 (2003).
2. Ashkin, A., Dziedzic, J. M., Bjorkholm, J. E. & Chu, S. Observation of a single-beam gradient force optical trap for dielectric particles. *Opt. Lett.* **11,** 288–290 (1986).
3. MacDonald, M. P., Spalding, G. C. & Dholakia, K. Microfluidic sorting in an optical lattice. *Nature* **426,** 421–424 (2003).
4. Grigorenko, A. N., Roberts, N. W., Dickinson, M. R. & Zhang, Y. Nanometric optical tweezers based on nanostructured substrates. *Nature Photon.* **2,** 365–370 (2008).
5. Born, M. & Wolf, E. *Principles of Optics* (Pergamon, 2003).
6. Almeida, V. R., Xu, Q. F., Barrios, C. A. & Lipson, M. Guiding and confining light in void nanostructure. *Opt. Lett.* **29,** 1209–1211 (2004).
7. Chiu, D. T. & Zare, R. N. Biased diffusion, optical trapping, and manipulation of single molecules in solution. *J. Am. Chem. Soc.* **118,** 6512–6513 (1996).
8. Hirano, K. *et al.* Sizing of single globular DNA molecules by using a circular acceleration technique with laser trapping. *Anal. Chem.* **80,** 5197–5202 (2008).
9. Psaltis, D., Quake, S. R. & Yang, C. H. Developing optofluidic technology through the fusion of microfluidics and optics. *Nature* **442,** 381–386 (2006).
10. Monat, C., Domachuk, P. & Eggleton, B. J. Integrated optofluidics: A new river of light. *Nature Photon.* **1,** 106–114 (2007).
11. Neale, S. L., Macdonald, M. P., Dholakia, K. & Krauss, T. F. All-optical control of microfluidic components using form birefringence. *Nature Mater.* **4,** 530–533 (2005).
12. Chiou, P. Y., Ohta, A. T. & Wu, M. C. Massively parallel manipulation of single cells and microparticles using optical images. *Nature* **436,** 370–372 (2005).
13. Liu, G. L., Kim, J., Lu, Y. & Lee, L. P. Optofluidic control using photothermal nanoparticles. *Nature Mater.* **5,** 27–32 (2006).
14. Wang, M. M. *et al.* Microfluidic sorting of mammalian cells by optical force switching. *Nature Biotechnol.* **23,** 83–87 (2005).
15. Sinclair, G. *et al.* Assembly of 3-dimensional structures using programmable holographic optical tweezers. *Opt. Express* **12,** 5475–5480 (2004).
16. Dholakia, K. & Reece, P. J. in *Structured Light and Its Applications* (ed. Andrews, D. L.) 107–138 (Academic, 2008).
17. Righini, M., Zelenina, A. S., Girard, C. & Quidant, R. Parallel and selective trapping in a patterned plasmonic landscape. *Nature Phys.* **3,** 477–480 (2007).
18. Marchington, R. F. *et al.* Optical deflection and sorting of microparticles in a near-field optical geometry. *Opt. Express* **16,** 3712–3726 (2008).
19. Cizmar, T. *et al.* Optical sorting and detection of submicrometer objects in a motional standing wave. *Phys. Rev. B* **74,** 035105 (2006).
20. Schmidt, B. S., Yang, A. H., Erickson, D. & Lipson, M. Optofluidic trapping and transport on solid core waveguides within a microfluidic device. *Opt. Express* **15,** 14322–14334 (2007).
21. Ng, L. N., Luf, B. J., Zervas, M. N. & Wilkinson, J. S. Forces on a Rayleigh particle in the cover region of a planar waveguide. *J. Lightwave Technol.* **18,** 388–400 (2000).
22. Grujic, K., Helleso, O. G., Hole, J. P. & Wilkinson, J. S. Sorting of polystyrene microspheres using a Y-branched optical waveguide. *Opt. Express* **13,** 1–7 (2005).
23. Gaugiran, S., Gétin, S., Fedeli, J. M. & Derouard, J. Polarization and particle size dependence of radiative forces on small metallic particles in evanescent optical fields. Evidences for either repulsive or attractive gradient forces. *Opt. Express* **15,** 8146–8156 (2007).
24. Ng, L. N., Luff, B. J., Zervas, M. N. & Wilkinson, J. S. Propulsion of gold nanoparticles on optical waveguides. *Opt. Commun.* **208,** 117–124 (2002).
25. Gaugiran, S. *et al.* Optical manipulation of microparticles and cells on silicon nitride waveguides. *Opt. Express* **13,** 6956–6963 (2005).

26. Yang, A. H. J. & Erickson, D. Stability analysis of optofluidic transport on solid-core waveguiding structures. *Nanotechnology* **19,** 045704 (2008).
27. Hart, S. J., Terray, A., Leski, T. A., Arnold, J. & Stroud, R. Discovery of a significant optical chromatographic difference between spores of *Bacillus anthracis* and its close relative, *Bacillus thuringiensis*. *Anal. Chem.* **78,** 3221–3225 (2006).
28. Svoboda, K. & Block, S. M. Optical trapping of metallic Rayleigh particles. *Opt. Lett.* **19,** 930–932 (1994).
29. Braslavsky, I., Hebert, B., Kartalov, E. & Quake, S. R. Sequence information can be obtained from single DNA molecules. *Proc. Natl Acad. Sci. USA* **100,** 3960–3964 (2003).
30. Woolley, A. T., Guillemette, C., Cheung, C. L., Housman, D. E. & Lieber, C. M. Direct haplotyping of kilobase-size DNA using carbon nanotube probes. *Nature Biotechnol.* **18,** 760–763 (2000).

**Supplementary Information** is linked to the online version of the paper at www.nature.com/nature.

**Acknowledgements** We thank A. Stroock for discussions, and A. Nitkowski and S. Manipatruni for technical support. This work was done in part at the Cornell NanoScale Facility, a member of the National Nanotechnology Infrastructure Network, which is supported by the US National Science Foundation. This work was funded by the US National Science Foundation NIRT: Active Nanophotofluidic Systems for Single Molecule/Particle Analysis (award number 0708599).

**Author Contributions** A.H.J.Y. and S.D.M. were responsible for running the bulk of the trapping experiments and analysing data. A.H.J.Y. carried out the simulation calculations. B.S.S was responsible for running initial experiments and fabrication of the slot waveguide chips. M.K. developed the DNA imaging methods. A.H.J.Y., M.L. and D.E. were responsible for writing the paper. All authors discussed the results and commented on the manuscript.

**Author Information** Reprints and permissions information is available at www.nature.com/reprints. Correspondence and requests for materials should be addressed to D.E. (de54@cornell.edu).